UDK 620.193:504.121:624.136.2:351.791.14 03
Original scientific article/Izvirni znanstveni članek

ISSN 1580-2949
MTAEC9, 55(4)491(2021)

ANTI-EROSION CAPACITY OF A GRANULAR FILTER SUBJECTED TO A PERIODICALLY VARIABLE HYDRAULIC GRADIENT

ODPORNOST GRANULIRANEGA FILTRA PROTI EROZIJSKI OBRABI, IZPOSTAVLJENEGA SPREMINJAJOČEMU IN IZMENIČNEMU HIDRAVLIČNEMU GRADIENTU

Yue Liang[1,2], Hongjie Zhang[1,2*], Xixi Shi[3], Chen Ma[1,2], Bin Zhang[1,2], Rifeng Xia[1,2], Lei Dai[1,2]

[1]National Engineering Research Center for Inland Waterway Regulation, Chongqing Jiaotong University, Chongqing, China
[2]School of River and Ocean Engineering, Chongqing Jiaotong University, Chongqing, China
[3]Local Maritime Office of Daying County, Sichuan, China

Prejem rokopisa – received: 2021-02-01; sprejem za objavo – accepted for publication: 2021-03-26

doi:10.17222/mit.2021.031

The instability of a filter system is a significant cause of seepage failure in embankment projects. The filter system in the earth-rock embankment is mainly composed of graded cohesionless soil. To uncover the performance of the granular filter in resisting the internal erosion, a set of experiments was carried out with an improved experimental apparatus, considering different hydraulic loading scenarios. The movement of graded cohesionless soil, the seepage velocity and the hydraulic gradient were monitored in the experiments. It was found that during the process of increasing the hydraulic gradient, the failure of the granular filter mainly experienced three stages: the first one was the dynamic equilibrium stage; the second was the critical start stage; and the third was the failure stage, in which a sudden change in the seepage velocity was the precursor of seepage failure. The critical hydraulic gradient and destructive hydraulic gradient decreased with the water level amplitude. Moreover, the experiments revealed that the loading modes of the hydraulic gradient significantly influenced the anti-erosion capacity of the granular filter. Compared with the stepwise loading mode, the cyclic reciprocating loading mode greatly weakened the anti-erosion capacity of the granular filter under the same water level amplitude. The destructive hydraulic gradient of the latter was only 71.8 % of the former under a higher water level amplitude, indicating that the corresponding measures should be considered to avoid the occurrence of a periodically variable hydraulic gradient.

Keywords: granular filter, hydraulic gradient, loading scenarios, anti-erosion capacity

Povzetek: Nestabilnost sistema za filtriranje je pomemben vzrok za pronicanje vode v projektih izgradnje nasipov oz. urejanja nabrežin. Filtrski sistem nasipa oz. obrežja je običajno zgrajen iz granuliranega kamenja, ki je v bistvu nekohezijska (nevezana, nasuta) zemljina. Avtorji tega članka so zato, da bi ugotovili lastnosti granuliranega filtra pred vplivom notranje erozije, izvedli vrsto eksperimentov z izboljšano eksperimentalno napravo, ki je omogočala izvedbo različnih scenarijev hidravlične obremenitve. Med preizkusi so sledili gibanju nesprijete (nekohezivne) zemljine, hitrosti gibanja nasipa in hidravličnemu gradientu (spreminjajočemu se nivoju oz. tlaku vode). S preizkusi so ugotovili, da med naraščanjem hidravličnega gradienta obstajajo tri faze oz. stadiji: prva faza je dinamični ravnotežni stadij, druga faza je kritični stadij pred začetkom puščanja in tretji stadij je stadij porušitve, pri katerem pride do nenadne spremembe hitrosti pronicanja, kar povzroči dokončno popuščanje/porušitev pregrade. Z zmanjševanjem amplitude nivoja vode se zmanjšujeta tudi kritični in rušilni hidravlični gradient. Nadalje so preizkusi pokazali, da načini obremenjevanja s hidravličnim gradientom močno vplivajo tudi na odpornost granuliranega filtra proti eroziji. Primerjava med postopnim naraščanjem obremenjevanja in izmeničnim obremenjevanjem je pokazala, da se pri slednjem načinu močno zmanjša odpornost filtra pri enakih amplitudah. Rušilni hidravlični gradient je bil pri izmeničnem obremenjevanju le 71,8 % tistega, ki ga je imel filter pri postopnem obremenjevanju. To pomeni, da je potrebno izvajati ukrepe, ki preprečujejo nastanek izmenično spreminjajočega se hidravličnega gradienta.

Ključne besede: granulirani filter, hidravlični gradient, obremenitveni scenariji, odpornost proti erozijski obrabi

1 INTRODUCTION

Embankment failure is one of the main causes of a catastrophic loss of life and property, especially in densely populated areas. For example, 62 dams in China's Henan Province were breached in an extreme storm, killing about 26.000 people in the region in August 1975.[1] Domestic and international data on embankment engineering accidents confirmed that about 40 % of the accidents were caused by internal erosion.[2,3] Recognizing the development mechanism of internal erosion is a crucial step in the risk assessment of embankment engineering. Studies on internal-erosion incidents were classified according to initiation mechanisms: concentrated leak erosion, backward erosion, contact erosion, and suffusion.[4,5] The studies on seepage erosion can be traced back to the early 1900s. The early studies mainly focused on the criteria for defining the onset of erosion. Some scholars proposed the criterion for calculating the critical head to define the effect of internal erosion.[6,7] On the basis of the critical hydraulic gradient used by Terzaghi to describe the critical state of cohesionless

*Corresponding author's e-mail:
zhanghongjie9601@163.com (Hongjie Zhang)

Table 1: Property parameters of the samples

Material name	d_{85} (mm)	d_{60} (mm)	d_{15} (mm)	d_{10} (mm)	D_{15} (mm)	D_{15}/d_{15}	D_{15}/d_{85}	C_u
Filter material	–	–	–	–	6.30	52.50	15.51	–
Base material	0.41	0.25	0.12	0.09	–	52.50	15.51	2.75

Note: D_{15} in the above table is the equivalent pore size of the filter layer

soil, other scholars continued to develop critical hydraulic gradient criteria to evaluate the occurrence and development of various internal erosion mechanisms.[8–10] The critical hydraulic gradient can be related to the intrinsic properties of soils and some external factors. In the past ten years, the effects of fine particle content, soil relative density, porosity, and other physical properties were widely studied through physical experiments.[11–13] Moreover, external factors such as stress state and seepage direction were also studied.[14,15]

To alleviate the disaster risk caused by seepage failure, the emergence of the filter layer brings a new opportunity to solve this problem. Filters are placed in the embankment body, its foundation, or other areas of hydraulic structures. Not only does a filter allow seepage water to pass freely, it also retains the soil particles of the base media. For the research on a filter layer, Terzaghi[16] proposed a well-known filter-retention criterion through engineering practice and a large number of laboratory tests in the early years. Sherard and Indraratna verified the effectiveness and applicability of Terzaghi's filter-retention criterion.[17] Although Terzaghi's filter-retention criterion is valid for uniform base media and filter media, there are still a few limitations for well-graded or uneven material. Based on the Terzaghi filter-retention criterion, the criterion and methods for determining the controlled soil-particle size for different types of seepage failure were further proposed, enlarging the application scope of the criterion.[18–20] A few numerical simulation techniques have been proposed in recent years with the computer-science development. The feasibility of the numerical model was validated by comparing the numerical-model results with some physical-experiment results.[21,22] A few scholars also carried out further research on the mesh division and solution method of the numerical simulation, improving the speed and accuracy of the numerical calculation.[23,24]

In hydraulic structures like dams and levees, cohesionless soil has been widely used as the filling medium, and the filter is often set as the seepage-proof measure. The structures are often exposed to complex hydraulic conditions such as the wave load and seasonal precipitation. The filter layer may become invalidated due to unqualified construction quality in the early stage. Even though the filter protection is set, the anti-erosion capacity of a granular filter has to be high due to complicated hydraulic conditions and an invalid filter. Therefore, this investigation uses an improved permeameter to study the influences of a periodically variable hydraulic gradient on the anti-erosion capacity of a granular filter, providing great significance to the safety of embankments.

2 EXPERIMENTAL PART

2.1 Materials

A rock-soil mixture was selected for the filter and base samples. It consisted of gravel or stone used as the filter medium and clay or sand used as the base medium. In this experiment, natural river pebbles were used as the filter medium, with particle diameters of (2–5, 5–8, 8–10) mm. Cohesionless fine sands were selected as the base media, with diameters of (0.075–0.25, 0.25–0.5, 0.5–1) mm, as shown in **Figures 1a** and **1b**.

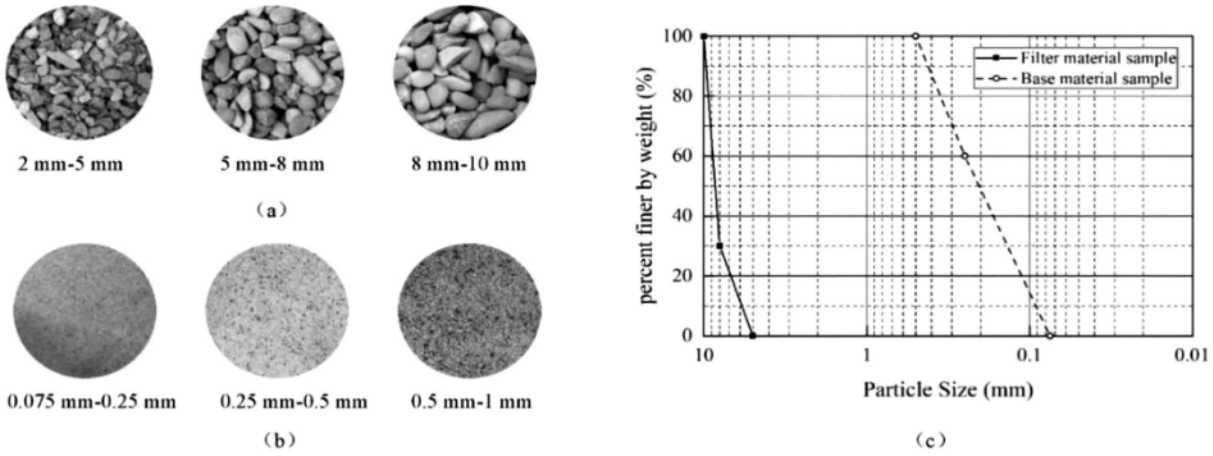

Figure 1: Materials used in the sample preparation: a) natural river pebbles, b) cohesionless fine sands, c) grading curve of the base and filter media

The basic physical properties of the cohesionless soil were tested; we determined an internal friction angle of 35°–39°, natural porosity of 0.36–0.42 and density of 1650–1750 kg/m^3. The grading curve in this experiment is shown in **Figure 1c**. Meanwhile, The effective and control grain sizes corresponding to the filter and base media are shown in **Table 1**.

2.2 Apparatus

The improved apparatus for seepage-failure experiments is shown in **Figure 2**. This apparatus is composed of a sample installation system, a hydraulic gradient control system, and a data acquisition system. The sample installation system consisted of a 300-mm diameter and 10-mm thick perspex glass chamber that could accommodate a 600-mm long test specimen, as shown in **Figure 2b**. Piezometer tubes with an inner diameter of 6 mm were designed to be placed at the water inlet and outside the sample cylinder. Two piezometer tubes on the outside had dimensions of 150 mm and 450 mm, and the bottom of the sample cylinder was selected as the datum. The bottom and outside of the sample cylinder were specially designed to prevent the outflow of the cohesionless soil by laying the filter layer. The inlet and outlet water funnels were provided with two overflow gaps and sealed screw caps to remove air from the sample cylinder during the sample saturation process. Besides, given the impact of the pressure head on the sample during the test, a spring plate was set at both ends of the sample cylinder, enabling the porous disc to come into close contact with the sample.

The hydraulic gradient control system was composed of a mobile air compressor, water-gas exchange-tank pressure-control cubicle, and downstream tank. On the upstream side, the air pressure provided by the air compressor is inputted into the pressure-control cubicle for adjustment and then outputted to the water-gas exchange tank, which can provide 0–1000 kPa water pressure to fully meet the test requirements. The downstream part controlled the height of the water tank through a lifting platform to adjust the required hydraulic gradient. It could be controlled within 200 mm to the maximum. Each part was connected with a 20-mm diameter acrylic pipe, as shown in **Figure 2a**.

The data-acquisition system comprised a piezometric tube panel, water-gathering barrel, electronic scale and stopwatch. The piezometric tube panel measured the hydrostatic pressure at three different locations. The water-gathering barrel collected the downstream water output per unit time. The mass of water output was weighed by an electronic scale to calculate its downstream outflow velocity as the average seepage velocity.

2.3 Experiment procedure

All the experiments involved three main steps. The first step was the filling of the sample. The filter and base media were poured into the sample cylinder 3–5 times. The thickness of each layer was measured with a steel ruler after the compaction to ensure that the particles were evenly distributed and not segregated during the filling process.

The second step was the saturation of the sample to expel air and fill all the voids in the sample with water. Saturation was achieved with the hydraulic gradient control system. This system allowed the water level in the sample to rise slowly from the bottom to the top. The

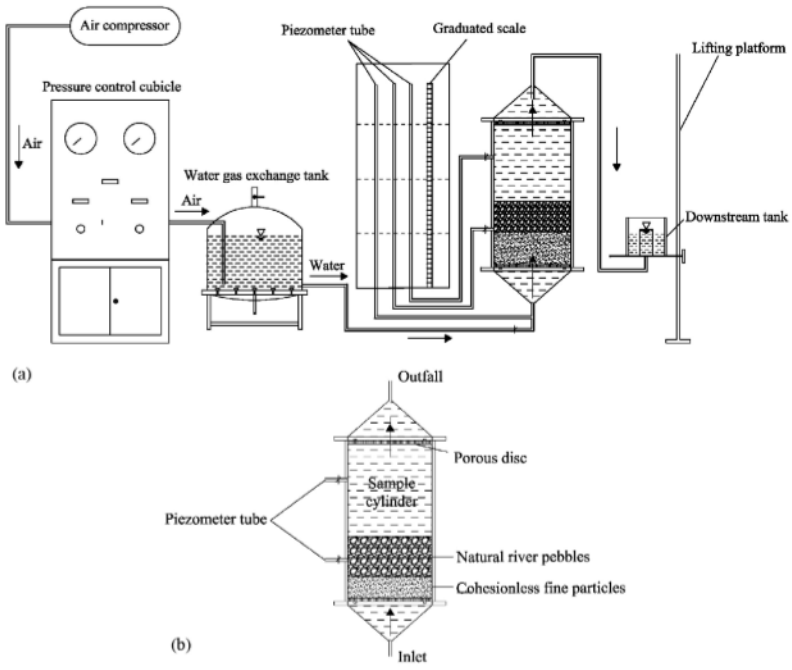

Figure 2: Sketch map of the apparatus: a) overall sketch of the apparatus, b) detailed map of the sample cylinder

water level passing through the sample was allowed to rise 2 cm each time to prevent a potential seepage failure. After the increase in the water level, the sample had to be allowed to stand still for 2 h. The total dwell time was not to be shorter than 4 h. The water level could be sequentially raised when the water level in the cylinder was stable and the soil below the water surface was completely saturated. Finally, the saturation was complete when the water overflowed from the downstream outlet.

The third step involved the realization of a seepage-failure experiment and an analysis of the anti-erosion capacity of the granular filter. For this purpose, the hydraulic gradient control system was used for applying the incremental hydraulic gradient to the sample. After the downstream water head was lowered by 5 cm, it had to remain stable for 10 min. Meanwhile, the flow rate (the flow rate was measured three times and the average value was computed to avoid an error due to the head instability) and the corresponding time were recorded. The increment of the gradient was stopped until the sample was damaged or the water head could not be lifted continuously.

2.4 Experiment schemes

Four sets of water level amplitude and two hydraulic gradient loading modes were used for the samples to investigate the influences of a periodically variable hydraulic gradient on the anti-erosion capacity of the granular filter. To isolate the effect of each factor, a set of experiments was performed on the samples with a given water level amplitude and different loading modes under the same conditions. All the scenarios are listed in **Table 2**. Experiments A1–A4 were conducted to investigate the effects of different water level amplitudes on the seepage velocity and hydraulic gradient of cohesionless-soil particles. The samples used in these experiments had the same particle-size distribution and filter thickness. Experiments B1–B4 used the same water level amplitudes as Group A. However, unlike Group A, which adopted the stepwise loading mode, Group B adopted the cyclic reciprocating loading mode of the water level amplitude. The purpose of Group B was to compare with Group A and explain the effect of different loading modes of the water level amplitude.

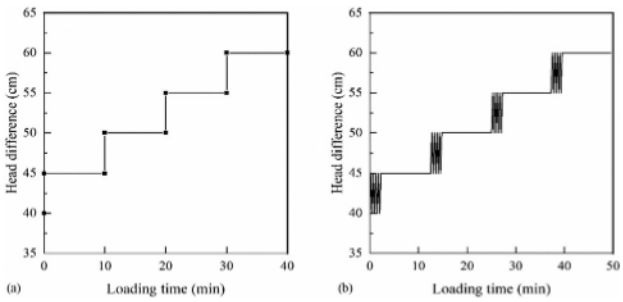

Figure 3: Two different loading modes: a) stepwise loading mode, b) cyclic reciprocating loading mode

Specifically, the stepwise loading mode refers to a gradual lowering of the downstream tank to a height specified each time in accordance with the specified water level amplitude, namely, a continual raising of the hydraulic gradient. Cyclic reciprocating loading means that the downstream storage tank is gradually lowered to a specified height and then raised again to the original height. The hydraulic gradient is adjusted by reciprocating five times at the same lowering and rising speed of 10 cm/min. The two multi-stage loading modes of the water level amplitude are shown in **Figure 3**.

Table 2: Summary of the general information about the experiments carried out in the study

Sample number	Filter-layer thickness (cm)	Load water level amplitude per level (cm)	Hydraulic gradient loading modes
A1	15	5	Stepwise loading mode
A2		10	
A3		15	
A4		20	
B1		5	Cyclic reciprocating loading mode
B2		10	
B3		15	
B4		20	

3 RESULTS

3.1 Cohesionless-soil-particle movement trends

The samples are divided into three layers from bottom to top, namely, the fine-particle layer, interface layer and filter layer. At the initial stage, the internal structure of a sample was stable, and the cohesionless-soil particles in the fine-particle layer were evenly distributed without any migration (**Figure 4a**). With the increase in the hydraulic gradient, the cohesionless soil was constantly impacted by the water flow. The cohesionless-soil particles began to move and the surface fine particles on the interface layer started to move up and down continuously, gradually moving away from the fine-particle layer and migrating inside the filter layer when the hydraulic gradient reached a certain level (**Figure 4b**). The number of the cohesionless-soil particles in the interfacial layer increased. Some of the cohesionless-soil particles were lost in the fine-particle layer, gradually forming a local preferential water-flow pathway with a continuous increase in the hydraulic gradient (**Figure 4c**). Subsequently, cohesionless-soil particles gradually penetrated the filter layer. Even if there was a filter-layer protection, the cohesionless-soil particles were eventually flushed out of the filter layer, causing seepage failure (**Figure 4d**).

According to the summary of the seepage-failure process, the whole test process can be divided into two or three phases. The first phase lasted from the beginning of the test to the dynamic equilibrium of the sample. The hydraulic gradient applied to the sample increased grad-

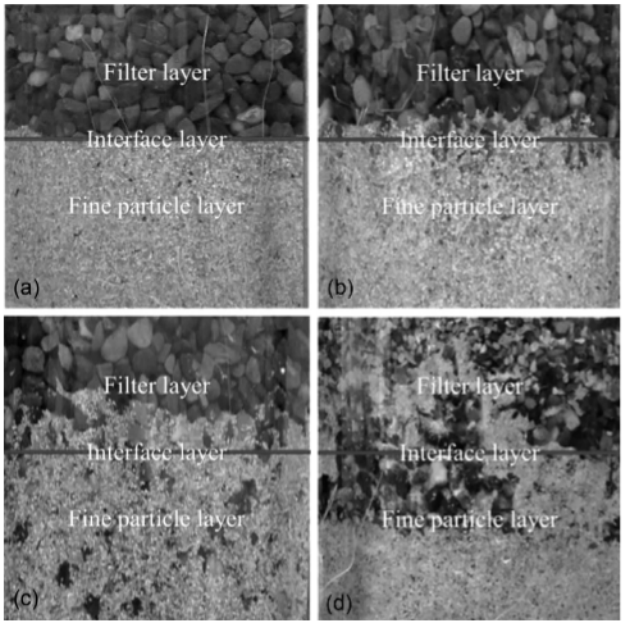

Figure 4: Particle migration paths: a) stable state; b) critical start; c) intrusion into the filter layer; d) being flushed out of the filter layer

ually in this phase, but the dynamic equilibrium of the cohesionless-soil particles was still maintained since the seepage force was relatively low. The second phase lasted from the stable state to the critical start of cohesionless-soil particles. The cohesionless-soil particles were gradually eroded, and the eroded fine particles were continuously carried into the filter layer by the water flow in this phase. In the third phase, many fine particles were flushed out of the filter layer by the fast-flowing water, and the whole sample was destroyed in a short time.

3.2 Changes in the seepage velocity and hydraulic gradient under the water-level amplitude

The water level in the test was changed by stepwise loading and was divided into four groups with different water-level amplitudes, namely Ha_1 = 5 cm, Ha_2 = 10 cm, Ha_3 = 15 cm and Ha_4 = 20 cm. Curves of the changes in the seepage velocity with the time is shown in **Figure 5a**. The seepage-velocity curves with the time for the four groups show that the particles are in a stable state at the initial time. A turning point appears on the curve with the increase in the test time. At this time, the sample reaches the critical starting state. Subsequently, fine particles enter the filter layer with the water flow, forming a seepage channel leading to seepage failure. Four sets of different water level amplitudes show that with the increase in the water level amplitude, the time for the particles of cohesionless soil to be flushed out of the filter layer gradually decreases. Meanwhile, the filter layer no longer serves as the buffer against seepage failure, and the anti-erosion capacity of the granular filter is almost completely lost due to large water level amplitudes. From the above phenomenon of the seepage test, it can be concluded that the surface particles start to pulsate continuously and reach the hydraulic gradient required for the critical start-up, called the critical hydraulic gradient i_c. Subsequently, the cohesionless-soil particles gradually enter the filter layer to form a seepage channel. The hydraulic gradient at this time is called the destructive hydraulic gradient i_d.

The critical hydraulic gradient and destructive hydraulic gradient of the sample underwent notable changes under different water level amplitudes. A double logarithm curve of the seepage velocity with the increase in the hydraulic gradient is shown in **Figure 5b**. During the first stage, the relations between the hydraulic gradient and the seepage velocity were linear, implying the stability of the cohesionless-soil particles based on Darcy's law on seepage. During the second stage, the increase in the seepage velocity accelerated when the hydraulic gradient exceeded the critical value. At this stage, fine particles with the water flow were observed in the filter layer as the hydraulic gradient increased continuously. In the third stage, the seepage velocity reached the relative maximum when the hydraulic gradient exceeded

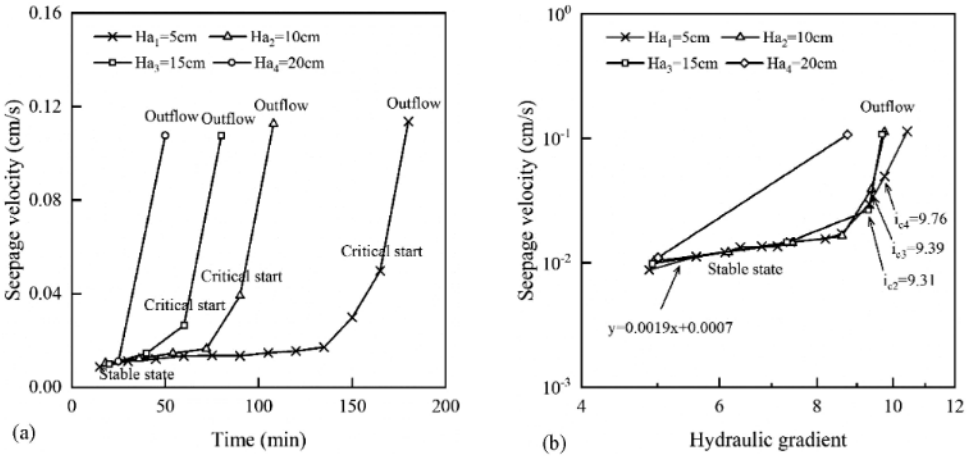

Figure 5: a) Curves of the seepage-velocity changes with time under different water-level amplitudes, b) influence of different amplitudes of the water level on the seepage velocity and hydraulic gradient

the destructive hydraulic gradient. At this point, cohesionless-soil particles were flushed out of the filter. Remarkably, there was no jump in the movement of the cohesionless-soil particles as it directly changed from a relatively stable state to rushing out of the filter when the water level amplitude was 20 cm. The relation curves of A1–A4 are nearly identical in all three stages. The first stage indicates the initial permeability coefficients of the cohesionless soil. The initial permeability coefficients of the four groups, fitted with the least square method, had an average of 0.0019 cm/s.

The turning point corresponding to the relationship between the seepage velocity and the hydraulic gradient is used as the critical value between the first and the second stage, which means that a sudden change in the seepage velocity is a precursor to seepage failure of cohesionless-soil particles. The critical hydraulic gradient of fine particles decreases from 9.76 to 8.75 with the increase in the water level amplitude. It is further clarified that the larger the water level amplitude, the earlier the cohesionless-soil particles reach the critical starting state, and the more sudden is the seepage failure.

Figure 6 shows the curves for critical hydraulic gradient i_c and destructive hydraulic gradient i_d under different water-level conditions. The results show that i_c and i_d decrease gradually with the increase in the water level amplitude. There is an obvious gap between i_c and i_d when the water level amplitude is lower. The gap between them becomes smaller and smaller; they tend to be almost the same when the water level amplitude is higher. This changing trend of hydraulic gradient also shows, once again, that the amplitude of the water level has an obvious influence on the anti-erosion capacity of a granular filter. With the increase in the water level amplitude, the hydraulic gradient required for cohesionless soil to reach the critical starting point and move out of the filter layer is smaller, and the time from the relative stability to the destruction of the cohesionless-soil particles is shorter.

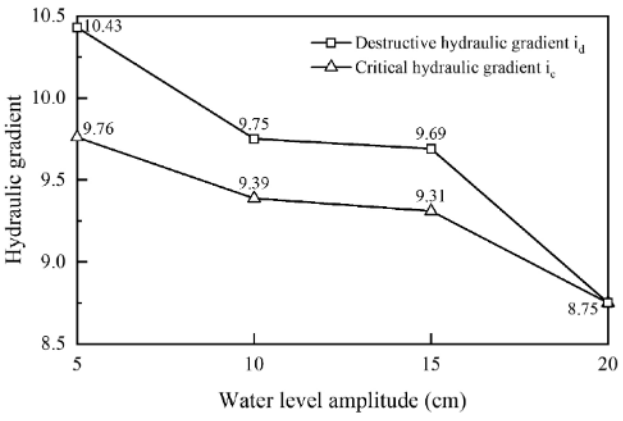

Figure 6: Changes in the critical and destructive hydraulic gradient with the water level amplitude (stepwise loading mode)

3.3 Influence of different loading modes for the hydraulic gradient on the anti-erosion capacity of the granular filter

The influence of the above water level amplitude on the anti-erosion capacity of the granular filter was discussed. The hydraulic gradient of tests A1–A4 was loaded using the stepwise mode. However, the hydraulic conditions of protection projects in practical engineering are often unstable. Therefore, the loading mode of a relatively complex hydraulic gradient, namely, the cyclic reciprocating loading mode is used when discussing the characteristics of the two different loading modes in this section. The hydraulic gradient of tests B1–B4 was loaded using the cyclic reciprocating mode. It was found that the migration law of cohesionless-soil particles is similar to that of tests A1–A4, which also had two or three stages in the testing process. Although the particle-transport laws under different loading modes are quite consistent, it is possible to identify some differences between them: only test A4 (Ha = 15 cm) in Group A did not go through the second phase; compared with Group A, B3 and B4 did not go through the second stage, but straight from the first stage to the third stage. When the water level amplitude was 15 cm, the fine particles in Test B3 remained relatively stable until the hydraulic gradient increased to 6.36. When the hydraulic gradient increased to 7.65, the fine particles moved with the direction of the water flow, and the fine particles in the interface layer moved slightly. When the hydraulic gradient increased to 8.32, a large deformation of seepage failure occurred and a seepage passage was formed.

It can be found from tests A1–A4 and B1–B4 that the influence of different hydraulic-gradient loading modes on the anti-erosion capacity of the granular filter is also significantly different under the same water level amplitude. **Figure 8** compares the hydraulic gradient and seepage velocity under two loading modes with the same water level amplitude. It can be seen that the critical hydraulic gradient of cyclic reciprocating loading mode is smaller than that of the stepwise loading mode, and the destructive hydraulic gradient of the former is also smaller than that of the latter, even at lower water level amplitudes of 5 cm and 10 cm. At higher water level amplitudes of 15 cm and 20 cm, it is more obvious that the two hydraulic gradients of tests B1–B4 under the cyclic reciprocating loading mode are smaller, the water level amplitude series experienced is reduced, and the test duration is shorter than for tests A1–A4. In terms of specific data, the gradient required for seepage failure in the cyclic reciprocating loading mode was reduced from 93.7 % of the stepwise loading mode to 71.8 %, showing a rapid declining trend. Compared with the stepwise loading mode, the cyclic reciprocating loading mode has a greater impact on the anti-erosion capacity of cohesionless soil so that a more abrupt seepage failure occurs, which is more difficult to prevent and control even with the protection of the filter layer.

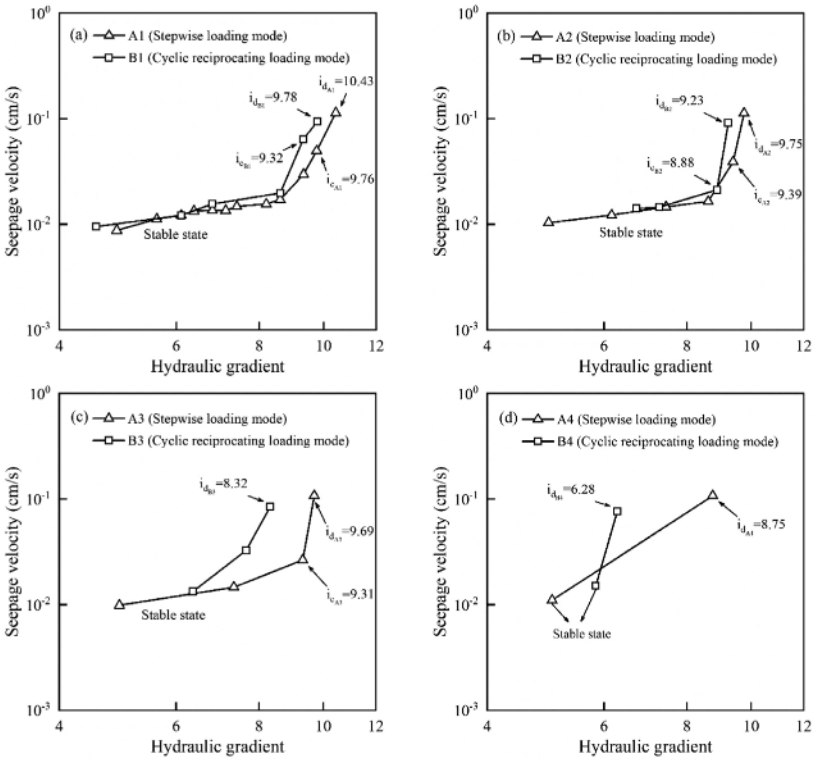

Figure 7: Comparison of seepage-velocity changes with the hydraulic gradient under different water level amplitudes with loading modes: a) Ha_1 = 5 cm, b) Ha_2 = 10 cm, c) Ha_3 = 15 cm, d) Ha_4 = 20 cm

4 DISCUSSION

The experiments revealed that the cohesionless-soil particles lose the anti-erosion capacity and flow out of the filter layer even under the protection of the filter layer due to the increase in the hydraulic gradient caused by the rising water level. It can be seen from the following classical Terzaghi filter retention criterion (Equations 1 and 2) that D_{15}/d_{15} of the materials used in this test is equal to 52.50, which allows a free passage of the seeping water through fine particles. However, this test simulated the invalid filter layer caused by poor construction quality. D_{85}/d_{15} of the test material is equal to 15.51; namely, the average pore diameter of fine particles is larger than the control particle size of the protected soil, which does not conform to the filtering principle. Therefore, none of the fine particles from the two groups could form a self-filtering and self-stable structure to prevent further migration of fine particles. This indicates that the invalid filter layer has a certain protective effect, but it cannot prevent a seepage failure, which is consistent with previous studies.[25,20]

$$D_{15}/d_{85} \leq 4\sim5 \quad (1)$$

$$D_{15}/d_{15} \geq 4\sim5 \quad (2)$$

The influence of different hydraulic gradient loading modes on the anti-erosion capacity of the granular filter is also significantly different under the same water level amplitude at each stage. The effect of dynamic water flow on the cohesionless soil at the cyclic water level is more obvious than the seepage under the water level caused by stepwise loading. Firstly, irrespective of the duration of the test or the specific values of the critical hydraulic gradient and destructive hydraulic gradient, as shown in **Figures 6** and **7**, Group B with cyclic reciprocating loading shows a more violent particle loss and weaker anti-erosion capacity. As the cohesionless soil exhibits dynamic stability under a low hydraulic gradient, it changes from being relatively stable to unstable with the periodic fluctuation of the hydraulic gradient, especially with a rapid hydraulic gradient increase.

Furthermore, the dynamic water flow continuously impacts the sample, which results in a rapid increase in the dynamic water pressure in the sample. The pore water pressure in the cohesionless soil cannot dissipate in time, resulting in a large amount of excess pore water pressure in the soil. On the one hand, the pore water pressure generated by the cyclic reciprocation of the hydraulic gradient causes a temporary increase in the local hydraulic gradient, which increases the seepage force, thus also increasing the erosion capacity of seepage.[26,27] On the other hand, with the increase in the seepage force, the amount of fine particles is smaller. Therefore, the critical hydraulic gradient under the cyclic loading of the water level amplitude is smaller than that under the step-by-step loading.

Secondly, the hydraulic gradient distribution in the soil is not uniform under circulating reciprocating water flow. The hydraulic gradient in the soil near the action boundary of circulating water flow is larger, while that in

the soil far away from the action boundary of circulating water flow is smaller. The boundary scouring is aggravated with a concentrated consumption of the impact energy on both sides of the soil. The energy after scouring flows further into the soil body due to repeated scouring of the boundary soil mass and soil-particle loss, which gradually causes the seepage failure. This phenomenon is worth noting in engineering practice.

5 CONCLUSIONS

A set of laboratory experiments was carried out using an improved apparatus to study the influence of hydraulic conditions on internal erosion, from which the following conclusions can be drawn:

The seepage failure mode of this experiment was contact erosion, and the erosion process can be divided into three stages. A sudden increase in the seepage velocity was the precursor of seepage failure, and even an invalid filter layer could mitigate the damage caused by the seepage failure under its protection. However, the invalid filter layer could not prevent the seepage failure, which was consistent with the previous studies. The critical hydraulic gradient and destructive hydraulic gradient for the seepage failure of fine particles decreased with the water level amplitude.

The damage made to the anti-erosion capacity of the granular filter by the two kinds of hydraulic gradient loading modes was almost the same under the action of a lower water level amplitude. Under a higher water level amplitude, the loss of fine particles due to the cyclic reciprocating loading was intensified. Its hydraulic gradient of failure was 71.8 % of that for the stepwise loading, indicating that the former was more likely to cause instability and destruction, and was harder to prevent.

In this test, homogeneous soils mixed with different particles were used as the test objects, but most of the soils in the actual engineering are inhomogeneous, making the process more complicated. Further research is needed to study the influence of hydraulic conditions on the anti-erosion capacity of a granular filter composed of inhomogeneous particles.

Acknowledgment

This work was supported by the National Key R&D Program of China (grant numbers 2019YFC1510802 & 2018YFB1600400), the National Natural Science Foundation of Chongqing, China (grant number cstc2018jcyjAX0559) and the Graduate Scientific Research Innovation Project of Chongqing, China (grant number CYS20291).

6 REFERENCES

[1] N. Ru, Y. Niu, Embankment dam incidents and safety of large dams, China Waterpower, Beijing 2001

[2] M. Foster, R. Fell, M. Spannagle, The statistics of embankment dam failures and accidents, Canadian Geotechnical Journal, 37 (**2000**) 5, 1000–1024, doi:10.1139/t00-030

[3] L. Zhang, Y. Xu, J. Jia, Analysis of earth dam failures: A database approach, Georisk, 3 (**2009**) 3, 184–189, doi:10.1080/17499510902831759

[4] R. Fell, J. J. Fry, The state of the art of assessing the likelihood of internal erosion of embankment dams, water retaining structures and their foundations, Internal erosion of dams and their foundations, Taylor and Francis, London 2007, 1–24

[5] R. Bridle, R. Fell, Internal erosion of existing dams, levees and dykes, and their foundations, Bulletin, 164 (2013)

[6] C. Ojha, V. Singh, D. Adrian, Determination of critical head in soil piping, Journal of Hydraulic Engineering, 129 (**2003**) 7, 511–518, doi:10.1061/(ASCE)0733-9429(2003)129:7(511)

[7] H. Sellmeijer, J. L. de la Cruz, V. M. van Beek, H. Knoeff, Fine-tuning of the backward erosion piping model through small-scale, medium-scale and IJkdijk experiments, European Journal of Environmental and Civil Engineering, 15 (**2011**) 8, 1139–1154, doi:10.1080/19648189.2011.9714845

[8] J. Israr, B. Indraratna, Study of critical hydraulic gradients for seepage-induced failures in granular soils, Journal of Geotechnical and Geoenvironmental Engineering, 145 (**2019**) 7, 04019025, doi:10.1061/(ASCE)GT.1943-5606.0002062

[9] Y. Liang, T. C. J. Yeh, Y. Zha, J. Wang, M. Liu, Y. Hao, Onset of suffusion in gap-graded soils under upward seepage, Soils and Foundations, 57 (**2017**) 5, 849–860

[10] D. S. Chang, L. M. Zhang, Critical hydraulic gradients of internal erosion under complex stress states, Journal of Geotechnical and Geoenvironmental Engineering, 139 (**2013**) 9, 1454–1467, doi:10.1061/(ASCE)GT.1943-5606.0000871

[11] L. Ke, A. Takahashi, Strength reduction of cohesionless soil due to internal erosion induced by one-dimensional upward seepage flow, Soils & Foundations, 52 (**2012**) 4, 698–711, doi:10.1016/j.sandf.2012.07.010

[12] M. S. Fleshman, J. D. Rice, Laboratory Modeling of the Mechanisms of Piping Erosion Initiation, Journal of Geotechnical & Geoenvironmental Engineering, 140 (**2014**) 6, 04014017, doi:10.1061/(ASCE)GT.1943-5606.0001106

[13] Z. Yao, J. Zhou, G. Zhang, B. Wu, Experimental study of particle grading impact on piping mechanism, J. Hydraulic Eng., 47 (**2016**) 2, 200–208, doi:10.13243/j.cnki.slxb.20150703

[14] Y.-H. Zou, Q. Chen, C.-R. He, J. Huang, Filter tests on gravelly soil and filter material under different stress states, Rock and Soil Mechanics, 33 (**2012**) 8, 2323–2329

[15] L. Ke, A. Takahashi, Experimental investigations on suffusion characteristics and its mechanical consequences on saturated cohesionless soil, Soils & Foundations, 54 (**2014**) 4, 713–730, doi:10.1016/j.sandf.2014.06.024

[16] K. von Terzaghi, Soil mechanics, a new chapter in engineering science, The 45th James Forrest Lecture, Journal of the Institution of Civil Engineers, 12 (**1939**), 106–142

[17] B. Indraratna, E. Dilema, F. Vafai, An experimental study of the filtration of a lateritic clay slurry by sand filters, Proceedings of the Institution of Civil Engineers – Geotechnical Engineering, 119 (**1996**) 2, 75–83, doi:10.1680/igeng.1996.28167

[18] B. Indraratna, A. K. Raut, Enhanced criterion for base soil retention in embankment dam filters, Journal of Geotechnical and Geoenvironmental Engineering, 132 (**2006**) 12, 1621–1627

[19] S. Jiang, Z. Fan, Application of reliability analysis to reverse filters design, Journal of Hydraulic Engineering, 39 (**2008**) 3, 295–300

[20] J. Liu, D. S. Xie, Design principles and guidelines of filters, Yantu Gongcheng Xuebao/Chinese Journal of Geotechnical Engineering, 39 (**2017**) 4, 609–616

[21] Q. F. Huang, M.-l. Zhan, J. C. Sheng, Y. l. Luo, B.-y. Su, Investigation of fluid flow-induced particle migration in granular filters using

a DEM-CFD method, Journal of Hydrodynamics, Ser. B, 26 (**2014**) 3, 406–415, doi:10.1016/S1001-6058(14)60046-9

[22] K. Cheng, Y. Wang, Q. Yang, A semi-resolved CFD-DEM model for seepage-induced fine particle migration in gap-graded soils, Computers and Geotechnics, 100 (**2018**), 30–51, doi:10.1016/j.compgeo.2018.04.004

[23] M. Wang, Y. T. Feng, G. N. Pande, A. H. C. Chan, W. X. Zuo, Numerical modelling of fluid-induced soil erosion in granular filters using a coupled bonded particle lattice Boltzmann method, Computers and Geotechnics, 82 (**2017**), 134–143, doi:10.1016/j.compgeo.2016.10.006

[24] Y. Liang, T.-C. J. Yeh, J. Wang, M. Liu, Y. Zha, Y. Hao, An auto-adaptive moving mesh method for the numerical simulation of piping erosion, Computers and Geotechnics, 82 (**2017**), 237–248, doi:10.1016/j.compgeo.2016.10.011

[25] Q. Chen, H.-H. Gu, C.-R. He, Combination seepage failure test of gravelly soil and the filter, Journal of Sichuan University: Engineering Science Edition, 44 (**2012**) 1, 13–18

[26] C. Rujikiatkamjorn, J. Israr, B. Indraratna, Laboratory Investigation of the Seepage Induced Response of Granular Soils under Static and Cyclic Loading, Geotechnical Testing Journal, (**2016**), doi:10.1520/GTJ20150288

[27] L. Chen, J. Zhao, G. Li, L. Zhan, W. Lei, Experimental study of seawall piping under water level fluctuation, European Journal of Environmental and Civil Engineering, 17 (**2013**) sup1, s1–s22, doi:10.1080/19648189.2013.834582